JOURNAL OF POLYMER SCIENCE Polymer Physics WWW.POLYMERPHYSICS.ORG REVIEW

Reversible Shape-Shifting in Polymeric Materials

Jing Zhou, Sergei S. Sheiko

Department of Chemistry, University of North Carolina at Chapel Hill, Chapel Hill, North Carolina 27599
Correspondence to: S. S. Sheiko (E-mail: sergei@email.unc.edu)

Received 6 November 2015; accepted 15 December 2015; published online 15 March 2016
DOI: 10.1002/polb.24014

ABSTRACT: In recent years, significant progress has been made in polymeric materials, which alter shape upon external stimuli, suggesting potential applications in robotics, biomedical engineering, and optical devices. These stimuli-responsive materials may be categorized into two classes: (i) shape-changing materials in which a specific type of shape-shifting is encoded in the original material structure and (ii) shape-memory materials, which do not possess any predetermined shape-shifting as prepared, yet allow programming of complex shape transformations on demand. While shape alterations in shape-changing materials are intrinsically reversible, shape memory is usually a one-way transformation from a metastable (programmed) to an equilibrium (original) state. Recently, different principles for both one-way reversible and two-way reversible shape memory have been developed. These offer a powerful combination of reversibility and programmability, which significantly expands the range of potential applications. The goal of this review is to highlight recent developments in reversible shape-shifting by introducing novel mechanisms, materials, and applications. © 2016 Wiley Periodicals, Inc. J. Polym. Sci., Part B: Polym. Phys. **2016**, *54*, 1365–1380

KEYWORDS: elastomers; hydrogels; liquid-crystalline polymers (LCP); polymers; shape memory; stimuli responsive

INTRODUCTION Shape-shifting materials change shape upon external stimuli, converting stored potential energy into motion as actuators. Since 1960s, shape-memory alloys have been widely used from biomedical and electronic engineering to aerospace industry.[1–5] Polymeric materials have also been intensively explored due to their low density, high deformability, and wide range of synthetic strategies in molecular design and functionalization for specific properties.[6–15]

Shape-shifting polymers can actively transform under a variety of stimuli including heat, electricity, light, solvent, and magnetic field.[16–22] The scale of shape alterations can range from macroscopic to micro- and nanometers.[23–30] Materials can be solid or swollen in a solvent (gels),[31–33] single- or multicomponent (mixtures, copolymers, composites).[23,34–36] And, various functions, such as biocompatibility and biodegradability, can be incorporated through chemical modifications to enable medical applications.[37–40]

Shape-shifting polymers is a specific class of stimuli-responsive materials, which can be divided into two subclasses as shape-changing and shape-memory materials.[41] A shape-changing material alters shape whenever a stimulus is applied, and returns to its original shape upon removal of the stimulus [Fig. 1(a)]. Typically, this results from thermal expansion, swelling, and phase transitions, that is, intrinsic material properties. As such, the material transits between two equilibrium states allowing for multiple shape-changing cycles without any external force. However, the type of shape transformation is predetermined by the original material structure and is usually limited to simple affine deformations. In contrast, shape-memory transformations are not inherently encoded within a material structure and require a programming step, upon which a sample is first deformed by an external force and then fixed in a temporary shape by a vitrification process (crystallization, glass transition, and gelation). This temporary shape is metastable and can be retained until an appropriate stimulus is applied to trigger recovery of the original equilibrium shape. Shape programming allows much more complex and versatile shape transformations. Multiple shapes can be memorized and recovered upon multiple stimuli in sequential order. Furthermore, the same object can be re-programmed to a new shape performing a different type of actuation on demand. However, a typical shape-memory transition is a one-way process, which is suitable for one-time application, otherwise requiring new programming after each cycle. Recently, new material designs and programming protocols have been developed to enable both one-way [Fig. 1(b)] and two-way [Fig. 1(c)] reversible shape memory (RSM) transformations.[42–49] This new class of materials significantly extends the range of practical applications for programmable shape-shifting.[50–52]

Jing Zhou is a postdoctoral researcher at the University of North Carolina at Chapel Hill, NC, USA, 2014. He received his Ph.D. in Materials Science from the University of North Carolina at Chapel Hill, 2014 and BS in Polymer Science and Engineering, from the Zhejiang University (China), 2008.

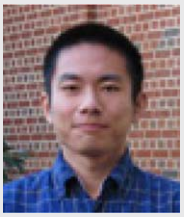

Sergei S. Sheiko is a distinguished Professor at the University of North Carolina at Chapel Hill, 2001-present; Fellow, American Physical Society, 2010; Habilitation in Polymer Chemistry at the University of Ulm, Germany, 2001; Postdoctoral Fellow at the University of Twente, The Netherlands, 1991-1993. He received his PhD in Polymer Physics from Institute of Chemical Physics of the Russian Academy of Sciences, 1991 and BS in Molecular and Chemical Physics from the Moscow Physico-Technical Institute, 1986.

SHAPE-CHANGING MATERIALS

Shape-changing materials undergo reversible shape alterations upon various stimuli. Generally speaking, nearly all objects change their dimensions in response to minute changes in the surrounding environment, for example, thermal expansion and swelling. Special materials were designed to perform particularly large expansion and shrinkage[53,54] in response to specific stimuli such as light and electromagnetic fields.[35,55–66]

In polymers, the most effective mechanisms for shape-changing include (i) swelling of gels controlled by solvent quality and crosslinking density,[67–70] (ii) photoisomerization of purposely introduced comonomers,[55–57,59,71,72] and (iii) liquid crystalline transitions.[73–77] In each case, shape alterations correspond to the corresponding equilibrium states of matter, where molecular-level interactions are transferred to the macroscopic level through networking. Most shape changes are isotropic, such as uniform volume expansion and shrinkage of pH responsive hydrogels demonstrated by Wu et al.[78] As shown in Figure 2, composite nanogels were prepared by *in situ* incorporation of CdSe quantum dots into the chitosan-poly(methacrylic acid) networks. The nano-gel exhibited significant shape shift due to pH-induced volume phase transitions of the chitosan-PMAA. These simple volume changes can control optical properties of sensors and regulate the releasing of drugs.

In addition to isotropic volume change, liquid crystalline (LC) materials allow for anisotropic shape transformations.[54,75–77,79–84] LC materials include loosely crosslinked LC elastomers with low T_g (<20 °C) and LC networks with elevated T_g, which show small-amplitude and fast shape changes. To enable correlation between LC ordering and macroscopic shape, polymer networks have been prepared by linking rod-like mesogenic groups through flexible spacers. In a nematic phase, polymer chains extend, while shifting to a random coil conformation upon a nematic-isotropic transition [Fig. 3(a)]. Anisotropic shape change requires objects possessing uniform orientation of the liquid crystalline domains within a polymer network. For this purpose, a multistep preparation process has been developed starting with loose crosslinking, which is followed by network deformation inducing ordering of the mesogens and then fixation of a permanent shape by completing network polymerization. Monodomain orientation of LC moieties ensures strong correlation between conformation of

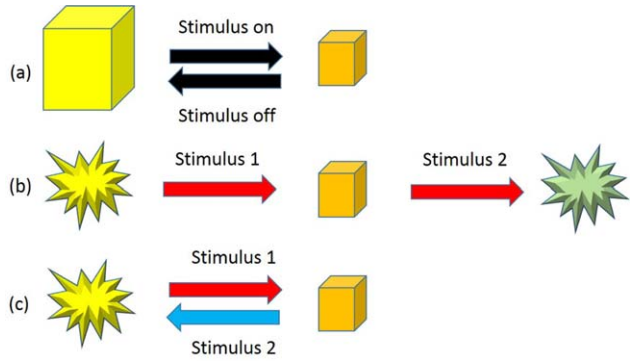

FIGURE 1 Reversible shape-shifting. (a) Shape-changing materials spontaneously change shape in response to an externally stimulus and return to the original shape once the stimulus is turned off. The shape change is inherent to a given material structure and usually allows only simple affine deformations. (b) Shape-memory transformations are not encoded in the material's structure and require programming through deformation and fixation of a temporary shape, which is retained until an appropriate stimulus is applied. This approach allows for complex and multiple shapes, which can be memorized and recovered in sequential order under different stimuli. Typically, shape recovery is a one-way transformation, yet it allows for shape reversibility as indicated by yellow and green shapes. (c) Two-way reversible shape-memory combines the reversibility of shape changing material and programmability of shape memory material. Two stimuli can be applied cyclically to induce reversible actuation for multiple times.

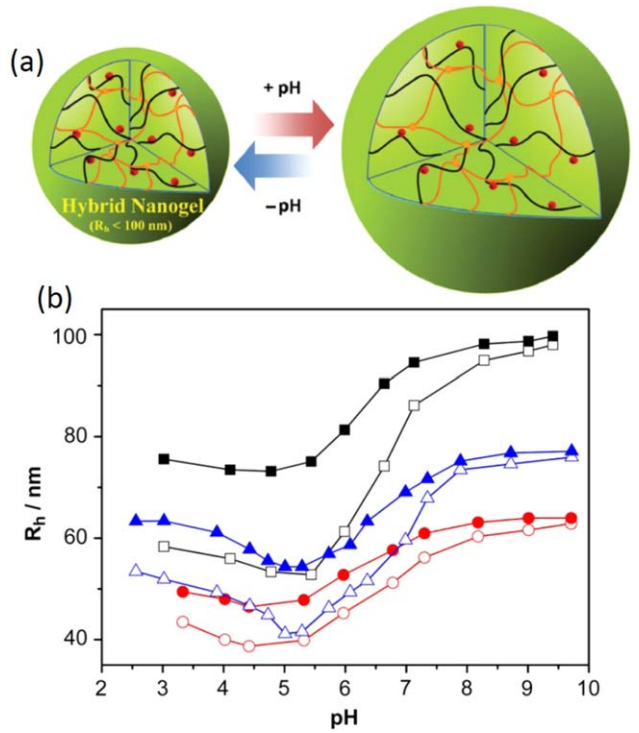

FIGURE 2 Ratiometric pH responsive hydro-gel with isotropic shape change. (a) Schematic of isotropic shape change in response to PH. (b) PH dependence of the average R_h (hydrodynamic radius) value of the chitosane PMAAeCdSe hybrid nanogels[78] (Reproduced from ref. 78, with permission from Elsevier Ltd.).

individual network strands and macroscopic shape of an elastomer sample [Fig. 3(b)]. As shown in Figure 3(c), LC elastomers allow for cyclic nematic–isotropic transitions cause anisotropic shape transformations, that is, elongation and contraction, in predetermined directions suggesting potential application as artificial muscles.[85–90]

Deformations of shape-changing polymers are predetermined by their original structure (chemical composition, molecular orientation, morphology, and shape). They are usually limited to simple expansion and contraction. Yet, more complex motions, such as bending and twisting, can be realized through composite design expanding the range of potential applications.[34,35,92–96] For example, a bilayer humidity sensor was developed by Dai et al. by depositing a shape-changing liquid crystalline material on a pre-extended elastic substrate.[92] The resulting bilayer composite allowed for significant bending in response to variations in humidity, while transferring simple expanding motion of the liquid crystalline layer into bending.

With the development of 3D-printing and nanoimprints, more sophisticated composite designs can be realized, allowing for more complex actuations with shape-changing materials. Wu et al. developed composite hydrogels that show three dimensional transformations such as twisting and coiling.[93] Upon variation in ionic strength, alternating domains with different swelling ratios and elastic moduli generate internal stress resulting cylindrical helices with equally probable right- and left-handedness [Fig. 4(a–c)]. Another approach to encode complex shape-shifting was proposed by Ware et al., who used photo-alignment of liquid crystal moieties to synthesize LCEs with imprinted 3D "voxels."[97,98] Each voxel undergoes 55% strain on heating with the direction of the strain dictated by the photo-alignment of the liquid crystal order. This enabled preparation of an elastomer with a complex LC alignment pattern, allowing for reversible shape transformations upon heating-cooling cycles [Fig. 4(d,e)].

SHAPE-MEMORY MATERIALS

In general, a shape-memory polymer is constructed of two networks. One network is a permanent chemical network supported by strong molecular crosslinks. This network controls a primary equilibrium shape. The other network is

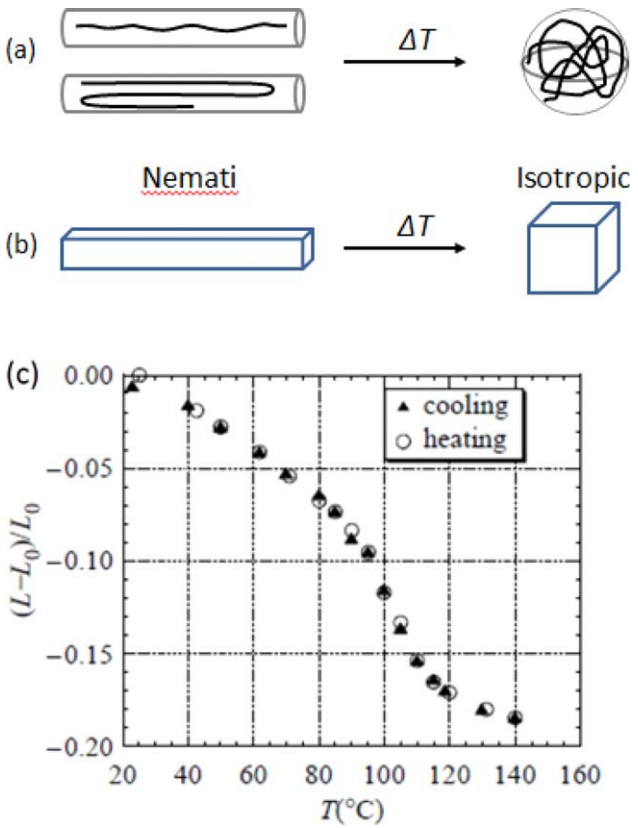

FIGURE 3 Liquid-crystalline material with anisotropic shape change (a) Conformations of main-chain LC polymers in the nematic (N) and isotropic (I) phases. In the nematic phase, depending on the molecular weight of the chain, two possible stretched chain conformations (linear and hairpin) were observed by neutron-scattering.[74,91] In the isotropic phase, a random coil (Gaussian-like) conformation was observed.[73] (b) Macroscopic shape change of the monodomain sample of main-chain LC elastomer at the nematic–isotropic transition.[85] (c) Contraction fraction $(L-L_0)/L_0$ as a function of temperature for LC elastomer[90] (Reproduced from ref. 90, with permission from Wiley).

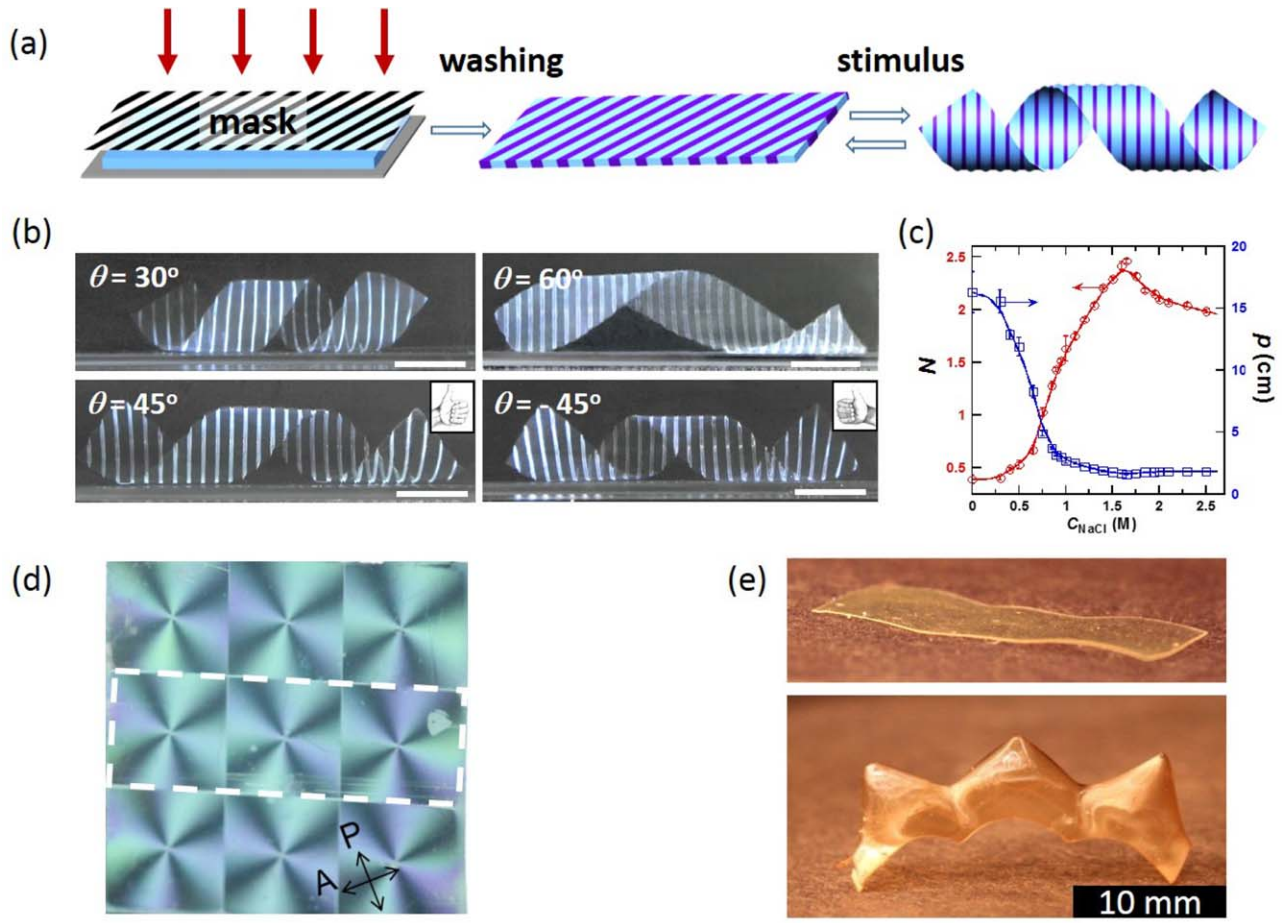

FIGURE 4 Formation of 3-D structure with composite polymer gel and voxelated LC elastomer. (a) Left: A planar sheet of the composite gel patterned with 1 mm-wide stripes of PNIPAm gel (PG) and PNIPAm/PAMPS gel (BG) passing at an angle θ to the long axis of the sheet. The dark and light-blue colors correspond to the stripes of PG and BG, respectively. Right: A helix formed by the composite gel sheet under the action of external stimulus. (b) Images of the helices generated from the gel sheets in a 1-M NaCl solution. The hand symbols indicate the handedness of the helix. The labels on the images show the value of angle θ. (c) Variation in pitch, p, and the number of turns, N, of the left-handed helix plotted as a function of the concentration of NaCl solution[93] (Reproduced from ref. 93, with permission from Nature Publishing Group). (d) Photograph of patterned LCE surface. (e) Upon heating, nine cones arise from the LCE film that reversibly flatten upon cooling[98] (Reproduced from ref. 98, with permission from The American Association for the Advancement of Science).

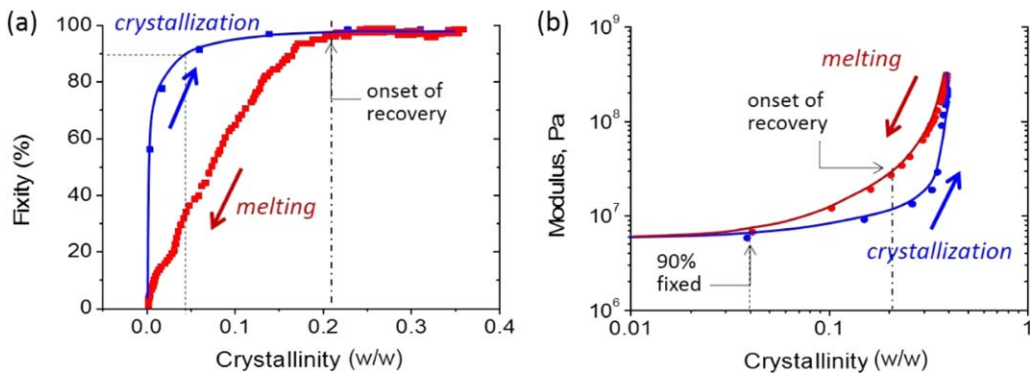

FIGURE 5 Shape control by a semicrystalline polymer. (a) Shape fixity (fixity$=\varepsilon_f/\varepsilon_p$, ε_p is programmed strain, ε_f is the fixed strain after releasing external force) in respect to different crystallinity. Only ~5% crystals are required for shape fixation. Difference in crystallization and melting due to different pathways that lead to different organization of crystals (b) Modulus change versus crystallinity shows the gradual change in materials properties in contrast with the sharp change in shape fixity.

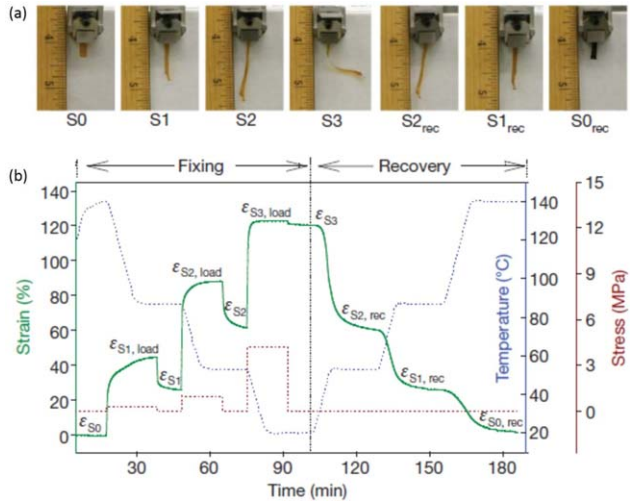

FIGURE 6 Multishape memory with temperature memory effect. (a) Images showing different programmed shapes (S0–S3) and multiple shape changes during recovery ($S2_{rec}$–$S0_{rec}$). (b) Quantitative mechanic cycle showing shapes were memorized and recovered corresponding to different programming temperatures[114] (Reproduced from ref. 114, with permission from Nature Publishing Group).

formed during programming process and supported by stimuli-responsive crosslinks of physical nature (crystallites, block-copolymer domains, and glassy clusters). While the first network provides an elastic restoring force ensuring recovery of the original shape, the second network is applied to fix the temporary shape for an extended period of time. The most typical mechanisms for shape fixation are glass transition and crystallization transition, while other types of vitrification mechanisms have been considered as well.[99–103] Shape-memory materials generally perform one-way transition between a temporary shape and its original shape. The temporary shape is fixed by stimuli-responsive crosslinks. This shape is metastable until an appropriate stimulus is applied triggering recovery of the thermodynamically more favorable state, while releasing the stored strain energy. Recently, new opportunities for shape memory polymers have been demonstrated by introducing the so-called 4D printing, which allows programming of complex shifts through self-assembly 3D-printed shapes extending this application to a "fourth" dimension.[104–108]

A distinct feature of shape-memory materials is programmability and capability of reprogramming the same sample to a different shape without altering the original molecular structure. Another important feature is that complex shapes can be fixed by incorporating a small amount of physical crosslinks. For example, less than ~5% crystallinity is required to fix a shape of a semicrystalline polymer (Fig. 5). This resembles shape control in jellyfish (composed of 95–98% of water and suggests high efficiency of a crystallization process in building a percolated scaffold of crystallites throughout an entire sample. Furthermore, additional crystallites forming at later stages of crystallization may be used for memorizing multiple shapes within a single programming process.[109] Similar concepts of multiple shape memory can be realized through other shape-fixation mechanisms (e.g., glass transition and hydrogen-bonding). The small amount of temporary crosslinks required for memorizing a single shape along with the ability to memorize different shapes with independent scaffolds lead to the potential of shape shifting between triple or multiple shapes in a single one-way shape memory transition.[109]

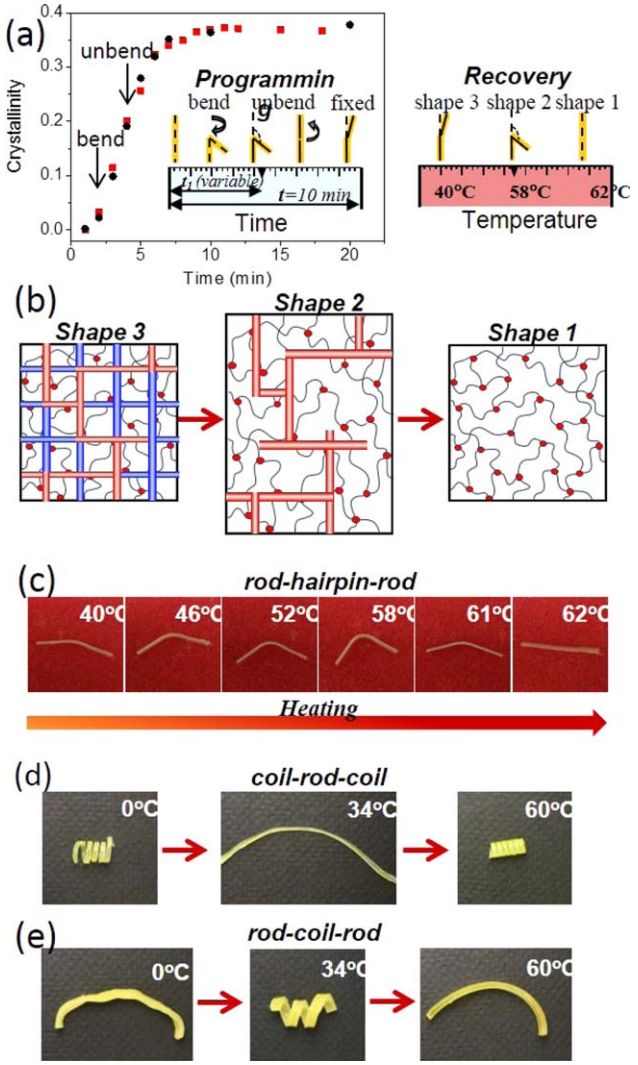

FIGURE 7 One-way reversible shaper memory (RSM) by isothermal programming. (a) For programming, a sample of poly(octylene adipate) polymer was cooled to 40 °C and bent to 180°. After time t_1 during crystallization at constant $T = 40$ °C, the sample was unbent to a straight ribbon shape for time t_2 until a total of $t_1 + t_2 = 10$ min was reached. During shape recovery upon heating, the sample bends and then unbends through heating. (b) Schematic of one-way RSM as different shapes memorized by distinct scaffolds of crystals. (c–e) One-way reversible shifting between complex shapes[48,109] (Reproduced from ref. 48, with permission from American Chemical Society and from ref. 109, with permission from Elsevier Ltd).

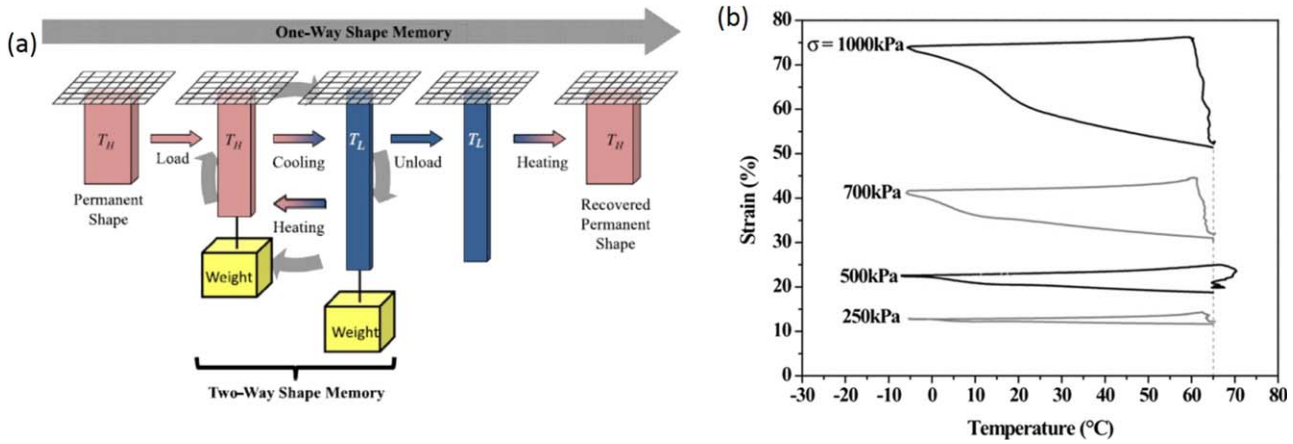

FIGURE 8 Two-way RSM with external force. (a) Schematic showing the difference between the one-way and two-way shape memory effects where T_H and T_L are temperatures greater than and less than the material's transition temperature. The top arrow represents the one-way shape memory transition while the circularly oriented arrows represent the repeatable, thermally controlled two-way RSM effect occurring due to a constant load[44] (Reproduced from ref. 44, with permission from IOP Publishing, LTD). (b) Two-way shape memory effect for PCL-T specimens subjected to a cooling-heating cycle and to various applied stresses[45] (Reproduced from ref. 45, with permission from Elsevier Ltd).

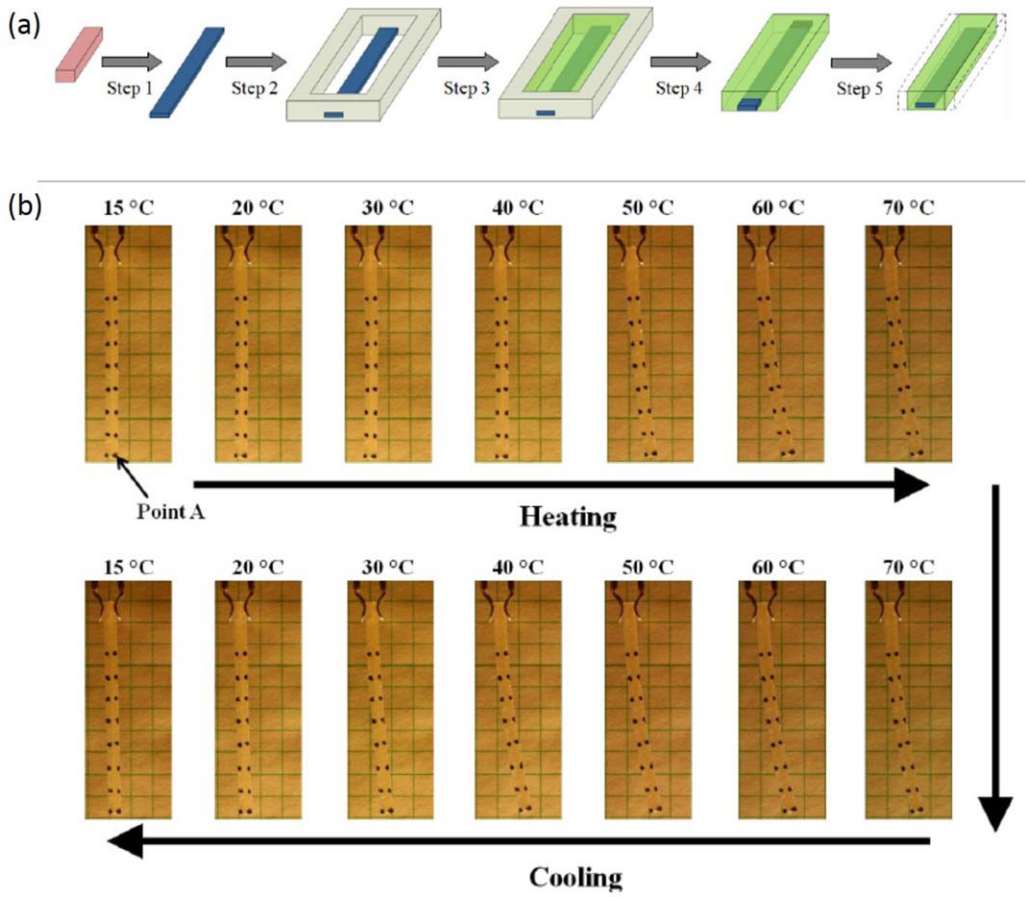

FIGURE 9 Free standing RSM composites (a) Schematic detailing the actuator fabrication process. (b) Actuator results for the first thermal cycle showing the free-standing two-way RSM effects[44] (Reproduced from ref. 44, with permission from IOP Publishing, LTD).

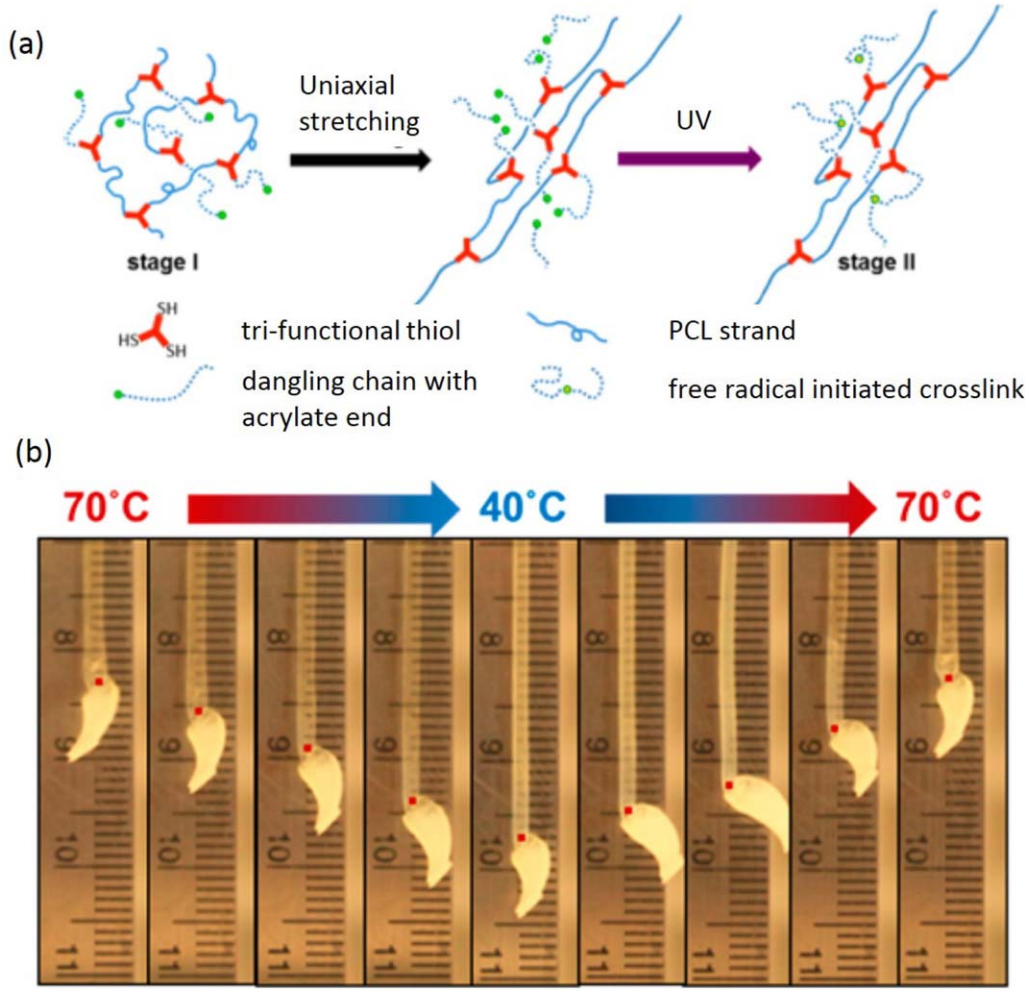

FIGURE 10 Dual crosslinking RSM (a) Cartoon showing preparation of dual-cure network stress free actuators. (b) A specimen with a gauge length of 8.3 cm, measured at 70 °C, under no external load, elongated to 9.7 cm, upon cooling to 40 °C, and reversibly returned to its initial length, upon heating to 70 °C[49] (Reproduced from ref. 49, with permission from American Chemical Society).

Triple Shape Memory and One-Way RSM

A variety of strategies have been developed for encoding triple or multiple shapes. One strategy requires the use of heterogeneous material such as block-copolymers and composites, in which each phase has a distinct crystallization and/or glass transition temperature. These two transitions have to be well-separated to allow two-step programming of two different temporary shapes by first cooling the sample below the first transition temperature to memorize the first temporary shape, which is followed by cooling the sample below the second transition temperature to memorize the second temporary shape.[110–113] The corresponding fixity ratios are determined by volume fraction of each component. Another approach for triple shape memory is based on the temperature-memory effect (TME), which suggests that materials have memory of the temperature at which the shape was programmed.[114–117] This approach requires polymers with a broad thermal transition (crystallization or glass formation), which allows programming of different shapes at distinct temperatures within the same thermal transition. The shape-memory performance (fixity ratio) is controlled by programming temperatures. Xie designed Nafion-based materials with particularly broad glass transition to demonstrate multishape memory effect.[114] During programming, multiple shapes were memorized at different temperatures allowing for sequential shape recovery corresponding to the programming temperatures (Fig. 6). Third method is based on isothermal crystallization, that is, programming different shapes at different times during crystallization at constant temperature.[109] This method relies on the kinetic nature of the crystallization process featuring sequential nucleation and growth of crystals, which enables fixation of different shapes at different stages of an isothermal crystallization process [Fig. 7(a)]. This strategy is analogous to a chemical aging study by Tobolsky and coworkers, in which two populations of network strands were introduced to be in equilibrium with deformed and original shapes respectively,[118] and could apply to semicrystalline materials with narrow crystallization and melting transitions. The fixation and recovery for different shapes can be modified by controlling the crystallization time.

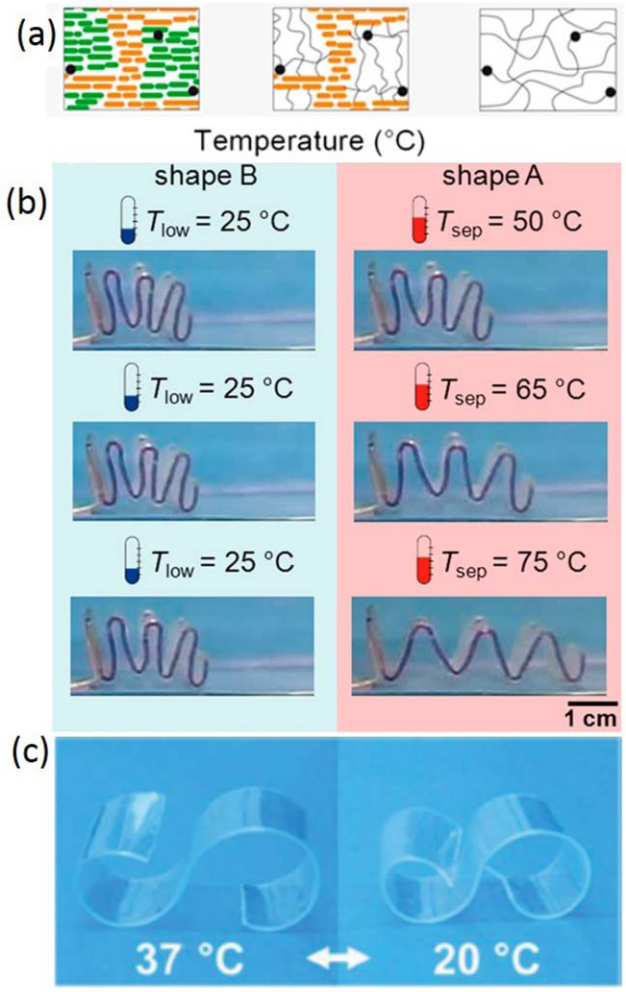

FIGURE 11 RSM based on temperature memory effect (a) Programming: Amorphous sample is deformed at T_{prog} (right); • chemical crosslinks. At T_{sep} (center) appearance is determined by the directed crystallization of the internal skeleton-forming domains (yellow). Actuation: reversible shape changes are realized in the polymer by crystallization/melting of oriented polyethylene segments in the actuation domains (green) between T_{low} and T_{sep} (left) (Reproduced from ref. 46, with permission from PNAS). (b and c) Photo series illustrating the temperature-memory[46,124] (Reproduced from ref. 124, with permission from Wiley).

Programming distinct shapes at different stages of a crystallization process suggests formation of individual scaffolds for each shape. It has been shown that newly formed crystals are able to fix a distinct shape independently of the presence of pre-existing crystallites.[109] This feature enables programming triple shape-memory effects at a single programming temperature. In one particular case, the third shape can be similar shape to the original primary shape. This type of programming enables reversible shape transformation as Shape 3 to Shape 2 to Shape 1, whereas Shape 3 is identical to Shape 1. As shown in Figure 7, heating of triple-shape programmed samples induces shape transformations in opposite directions (bend-unbend, coil-uncoil), which occur sequentially in one heating process.[48] Even though Shape 3 is macroscopically identical to the original shape (Shape 1), the material inside these shapes undergoes irreversible transitions between microscopically different metastable structures toward an equilibrium one. Hence, this one-way shape transformation can be viewed as pseudo-reversible.

Two-Way RSM Materials

Shape-memory cycles are usually irreversible, as they are driven by relaxation of polymer network strands from metastable to equilibrium materials structures. Therefore, it is challenging to reverse the course of material relaxation and, thus, make shape memory reversible. One way to confront the equilibration process of network relaxation is to apply an external force. The other way is to design materials that generate an internal force opposing recovery of a primary shape.

The first RSM behavior was reported in semicrystalline polymer networks under external load.[42] A typical force-mediated RSM cycle is shown in Figure 8(a). In the programming step, a sample is initially stretched at a temperature above the transition temperature (T_t) under a constant tensile load. After cooling below T_t while maintaining the external load, the sample shows significant elongation called cooling induced elongation (CIE). Subsequent heating above T_t causes the sample to shrink to its initial shape. This phenomenon has been later demonstrated for different polymer systems.[43,45,119] Two mechanisms contribute to the reverse shape variation under external load. First is the entropic rubber elasticity with shear modulus $G=\nu RT$, where ν is the crosslinking density, R is the universal gas constant, and T is the absolute temperature. Upon cooling, a decrease in modulus causes an increase in elongation, while a reverse behavior is observed during heating. Second, upon crystallization, the shape further changes due to stretch-induced crystallization (SIC), which is preferentially taking place along the loading axis.[45] The extent of elongation and contraction can be controlled by the applied external load: larger load leads to more stretched chains and more significant SIC resulting in larger deformations [Fig. 8(b)].

A permanently applied external load imposes a significant limitation for complex shape transformations. In general, free-standing materials that allow two-way RSM are desired for many applications. This can be accomplished by incorporation of stress-applying component either through object design (composites) or material design (heterogeneous networking). Polymer composites with free standing two-way reversible actuations have been recently developed.[44,120–123] Westbrook et al. demonstrated an example of embedding a shape-memory polymer in an elastic polymer shell, which exerts restoring stress on the semicrystalline shape-memory core. The fabrication of a two-way reversible polymer composite is shown in Figure 9(a). Step 1: the shape memory polymer (PCO–DCP) strip is programmed at temperature above the melting transition (T_H) and its shape is fixed below the crystallization transition (T_L); Step 2: the

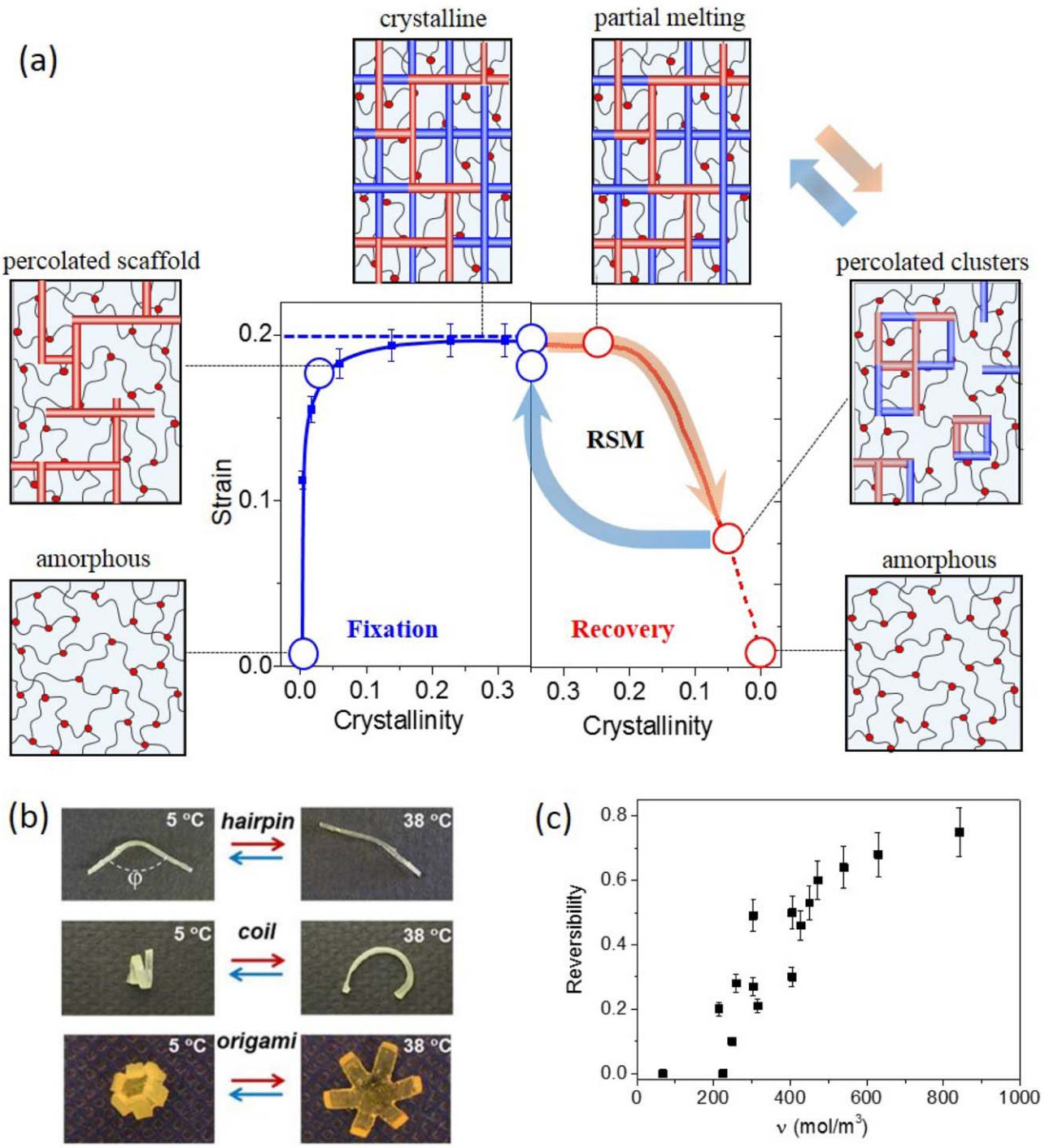

FIGURE 12 Semicrystalline RSM polymer based on confined crystallization. (a) A programing strain of $\varepsilon_p = 20\%$ is applied to sample at 80 °C and then fixed by quenching to 0 ° C. Each data point in the fixation panel corresponds to a strain fixed (ε_f) by quenching at a given stage of the crystallization process. A percolated crystalline scaffold is developed. Crystals in black color indicate early stage in fixation, blue color indicate the rest "redundant" crystals in fixation. Upon melting, the crystalline scaffold is melted into percolated clusters. At any stage of the melting process, heating can be switched to cooling and reverse the shape transformation from ε_h to ε_c. (b) Examples of two-way RSM: hairpin, coil, and origami.[48] (c) Reversibility (reversibility$=(\varepsilon_c\text{-}\varepsilon_h)/\varepsilon_f$) affected by crosslinking density (Reproduced from ref. 48, with permission from American Chemical Society).

programmed strip is mounted inside the custom-manufactured mold; Step 3: the matrix material is injected inside the mold and photo-cured; Step 4: the mold is thermally cured and the presectioned actuator is removed; Step 5: the actuator is sectioned to the required geometry. Reversible shape changes have been shown in Figure 9(b).

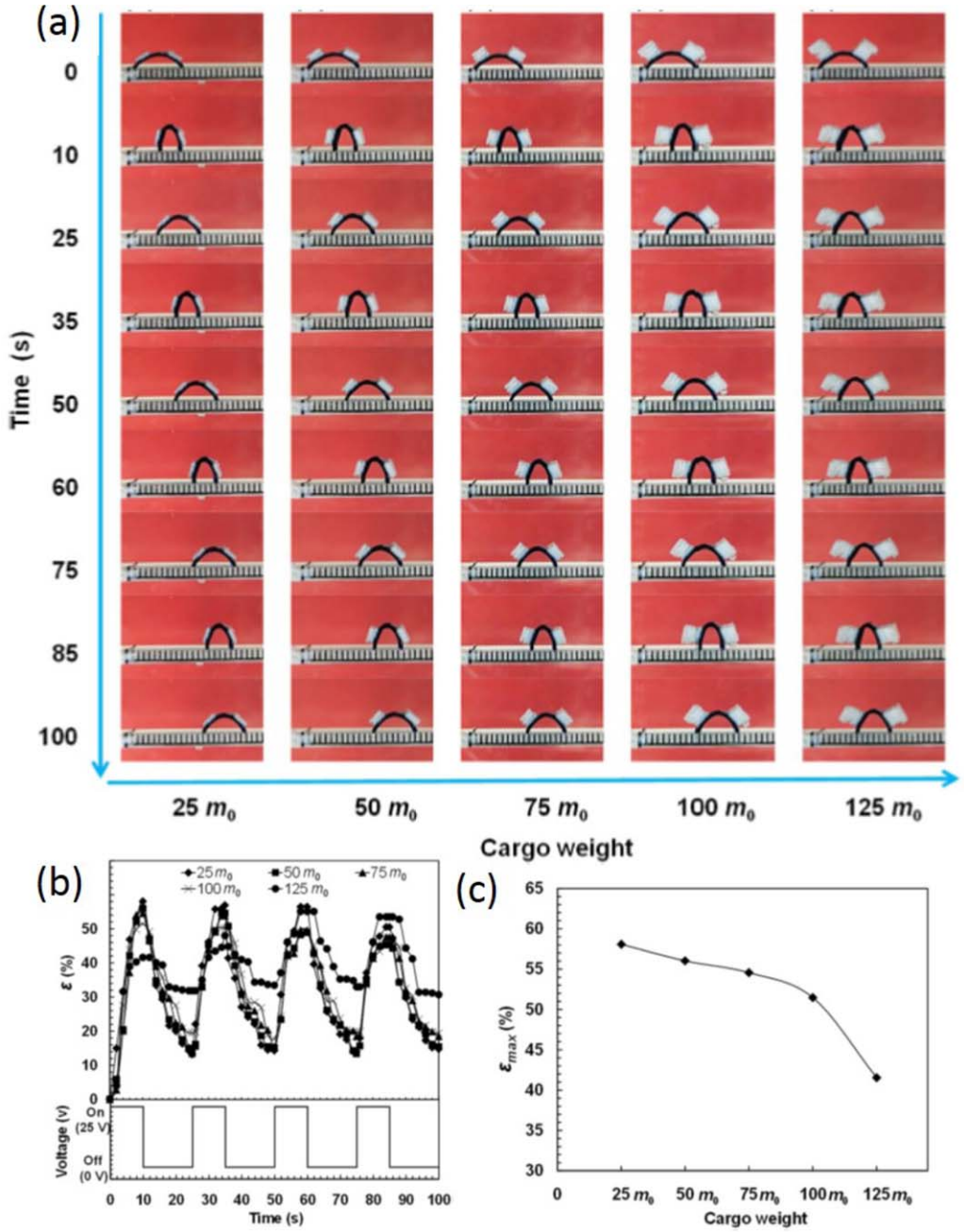

FIGURE 13 Cargo carrying microrobotic. (a) Photographs showing the walking behaviors of hydrogel walkers loaded with different weights of cargo. (b) Bending behaviors of the hydrogel walkers loaded with different weights of cargo during the electro-induced walking. (c) Effect of cargo weight on the maximum ε of the hydrogel walkers[63] (Reproduced from ref. 63, with permission from Nature Publishing Group).

During heating, the shape-memory core contracts toward its original shape, bending the sample and storing elastic stress in the deformed elastic outer shell. During cooling, CIE of the core was induced by the stress of the shell and the sample straighten up to the original state and such actuation could be repeated for multiple cycles.

This mechanism was extended to one component materials possessing dual network architectures.[49] In this case, RSM was realized through two stage curing process, which is analogous to the liquid crystalline shape-changing materials. A partially crosslinked, semicrystalline poly(ε-caprolactone) (PCL) network is melted, stretched to several hundred percent strain, and then fully crosslinked [Fig. 10(a)]. When the load is removed above the melting temperature, the network is unable to retract to its original unstrained state, while adopting a metastable "state-of-ease," which balances elastic stress from the original, load-bearing network strands with

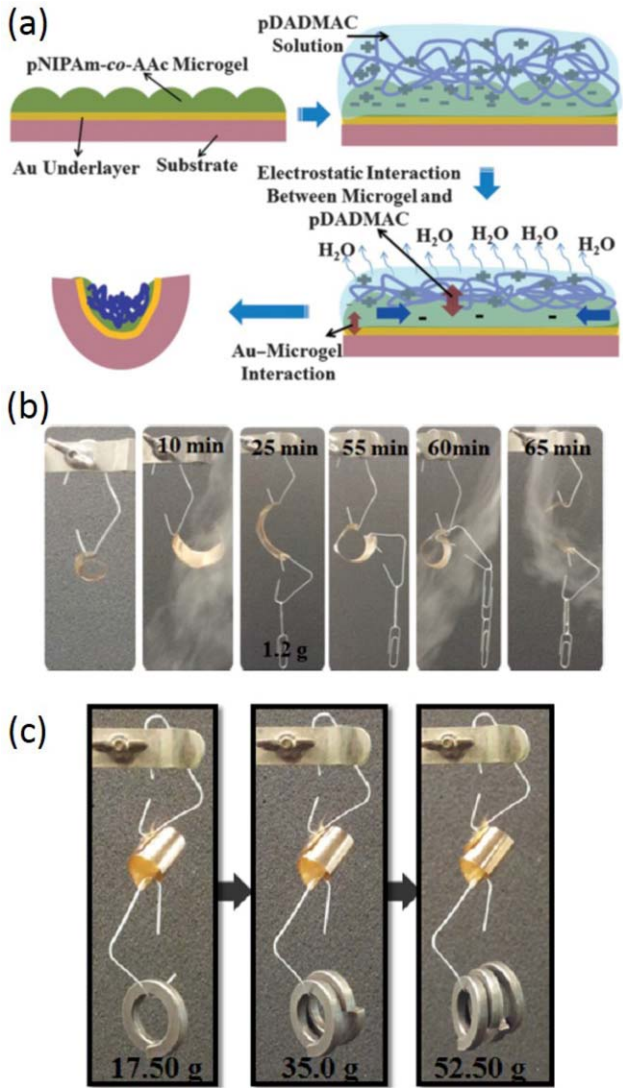

FIGURE 14 Artificial muscles. (a) A flexible plastic substrate was coated with an Au/Cr layer. PNIPAm-*co*-AAc microgels were deposited on this substrate, Addition of a pDADMAC solution renders the pNIPAm-*co*-AAc microgel negatively charged owing to the deprotonation of AAc moieties in the microgel initiating the electrostatic interaction between the microgels and polyelectrolyte. Upon drying, the pDADMAC layer contracts bending the substrate owing to the strong interactions between the microgels and pDADMAC and the microgels and Au. (b) A small curled substrate was hung from an arm and cycled between low and high humidity. (c) A dry polymer-based device resisting uncurling as masses are hung from the end of the device[87] (Reproduced from ref. 87, with permission from Wiley).

the entropic stress from newly formed sub-chains. Upon cooling, internal stress between the two networks facilitates crystallization, which causes further elongation of configurationally biased chains. When heated, crystallites melt, and the sample returns to its equilibrium state [Fig. 10(b)]. Two-way shape actuation can be performed upon cyclic heating and cooling.

Internal anisotropic stress can be also generated during conventional polymer crystallization provided that a crystallization process is molecularly controlled (hindered, constrained, and directed). Behl et al., demonstrated two-way RSM with materials of two crystalline domains.[46,47] The two domains of different transition temperatures determine the two shapes the sample can actuate in between. Programming of a shape shift begins with macroscopic deformation under external force to the desired shape in the rubbery state where all chain segments are stretched and orientated. The sample is then fixed at T_{low}, a temperature where all the crystallizable segments are crystalized. Upon heating to T_{high}, which is between the transition temperature of two domains, the sample shifts to shape A. Subsequent crystallization of the oriented actuator segments by cooling to T_{low} results in shape B. Reheating to T_{high} causes the actuator domains to melt and reversibly shift back to Shape A. This reversible shape change through heating and cooling cycle between T_{low} and T_{high} can be repeated several times (Fig. 11). At temperature $T_{high,}$ the high transition temperature domains provide a scaffold, which is both elastic and capable of exerting internal stress to trigger stress-induced crystallization (SIC) of chains at a lower temperature. The difference in transition temperatures can be realized in either multicomponent materials (e.g., copolymers and composites) or single-component systems through the temperature memory effect, which differentiates crystals with distinct programming temperatures.

Another general approach for two-way shape memory is based on kinetically preferred pathways of self-seeding crystallization, which can be applied to conventional semicrystalline polymers with narrow transitions.[48,125] As shown in Figure 12(a), the protocol of programming is similar to conventional shape memory with a percolated crystalline scaffold that secure the temporary shape. Upon melting, the scaffold loses its percolation allowing for shape recovery. Heating can be stopped at any partially molten state, while subsequent cooling and recrystallization leads to reverse shape-shifting. The reversed direction is explained by the kinetic nature of crystallization which is strongly biased by topological constraints imposed by chemical crosslinks and remaining crystallites. Replicating the original scaffold is the fastest pathway for recrystallization, which causes chain extension in the amorphous phase and reinstallation of the programmed shape. This approach has no limitations in terms of shape type and programming of reversible complex shape-shifts such as bending, twisting, and origami folding [Fig. 12(b)].

The reversible shape actuation is caused by the interplay of two networks at $T_{partial}$: (i) the chemical network, which is partially released and (ii) the crystalline scaffold, which is partially removed. While competing, both networks provide topological constraints for the polymer strands that both hinder and direct the recrystallization process. Reversible strain fraction is controlled by partial melting temperature. Increasing $T_{partial}$ allows for larger strain recovery due to chemical network relaxation; however, it also results in

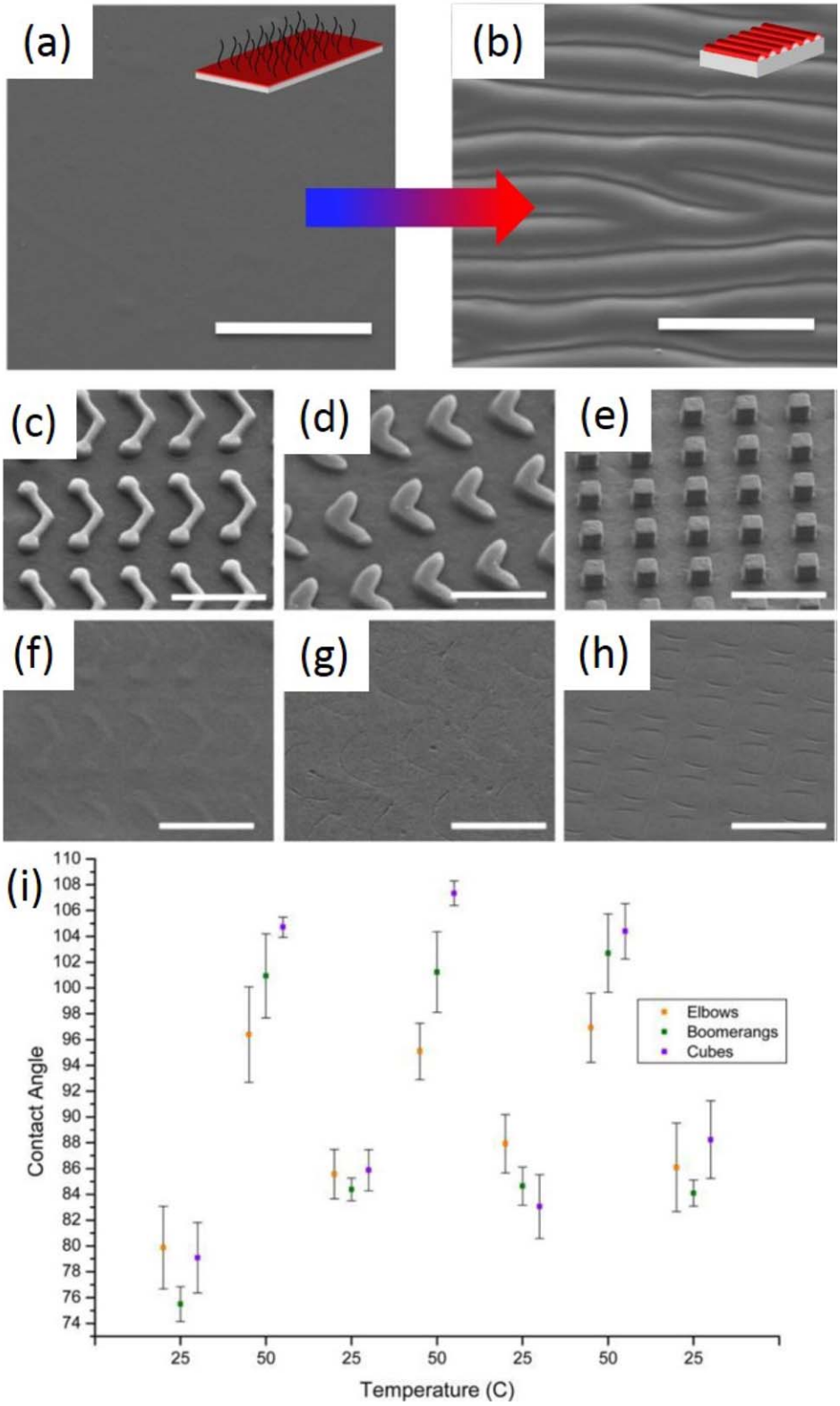

FIGURE 15 Dynamic surfaces. (a and b) Wrinkles formed through shape shifting. (a) Wrinkles formed after shape recovery from flat temporary shape. (b) Schematic of wrinkle formation on brush grafted substrates[137] (Reproduced from ref. 137, with permission from American Chemical Society). Reversible micropatterns. SEM images of surfaces embossed with (c) boomerangs, (d) elbows, and (e) cubes in their equilibrium states, and (f−h) the same surfaces after programming into their metastable states.(i) Contact angles reversibly modulated by repeated heating and cooling between $T = 25$ °C and $T = 50$ °C[50] (Reproduced from ref. 50, with permission from American Chemical Society).

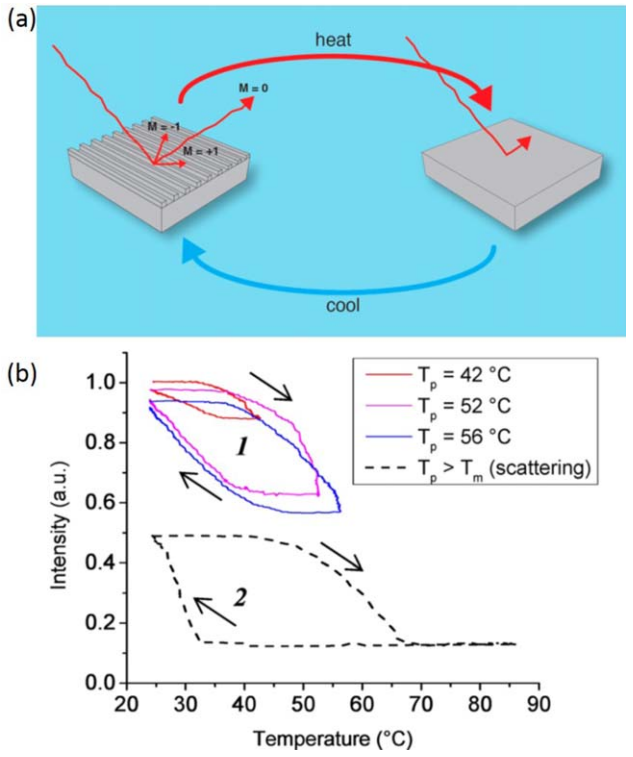

FIGURE 16 Dynamic optical grating. (a) Reversible shifting of the grating height was accomplished through partial melting and recrystallization of semicrystalline poly(octylene adipate). (b) Optical intensity of a diffraction spot as temperature was varied (arrows showing ramping direction). Region 1: Optical intensity can be reversibly controlled within different cycles with T_p kept below T_m. Region 2: When T_p is increased above T_m, the grating is greatly erased and nonrecoverable. The intensity drops significantly as the temperature increases to T_f ($T_f = 70$ °C). Now the surface returns to its flat primary shape and the intensity changes upon cycling are due to melting/crystallization-induced scattering[51] (Reproduced from ref. 51, with permission from American Chemical Society).

melting of the scaffold, which holds memory of the temporary shape, allowing random recrystallization. Note that the constraint chains can slowly reorganize and relax during annealing at $T_{partial}$. This relaxation can be significantly hindered by increasing chemical crosslinking density up to a time scale of the order of days. As shown in Figure 12(c) reversibility of more than 70% of the original strain can be achieved by tuning the crosslink density. Network topology also affects reversibility, but in a less dominant way then crosslink density.

APPLICATION

Micro Robotics

The shape shifting of polymers is accompanied by force generation, converting stimuli into mechanical energy. With elaborated designing, the samples are able to perform remote manipulated self-locomotions as microrobotics.[62,63,126–129] By applying cyclic stimuli, the reversible deformation of bending and unbending can be transformed into motions such as swimming or walking. Yang et al., designed the cargo carrying microrobotic with electroactive hydrogel.[63] Under electric fields, the polyelectrolyte networks can achieve asymmetric swelling/shrinking volume changes as well as bending behaviors, due to the osmotic pressure difference induced by electric-field-driven ion motion. Via repeated "on/off" electro-triggering cycles, the hydrogel walkers can move their two "legs" to achieve one-directional walking motion and transportation of cargoes (Fig. 13).

Biomedical Devices and Artificial Muscles

Polymeric materials may offer multiple functionalities including biocompatibility or biodegradability which make them appealing candidates for biomedical devices. Mechanically smart polymers that can shift shape have large potential in biomedical applications. For example, in minimally invasive surgery, shape shifting stents can be designed to prevent vasospasms. The stent can be inserted or removed as thin wires and expand *in situ* under stimuli.

Mimicking the human muscles that convert contraction and extension into weight lifting motions, a variety of polymeric artificial muscles has been developed.[85–90] Figure 14 demonstrates a bilayer composite with humidity sensitive polymer gels that bend and unbend in response to the humidity change. Weight can be lifted in repeated cycles mimicking muscles contractions.

Shape Changing Substrates

Shape-shifting materials can perform shape variations from macroscopic to micro/nanoscales. Dynamic change in surface topologies and microstructures can affect physical properties including wetting, adhesion and propulsion effects.[130–134] Specific microfeatures can also be prepared through shape change.[135–137] Figure 15(a,b) demonstrates the wrinkles formed in the shape recovery process utilizing a shape-memory polymer (poly(octylene diazoadipate-*co*-octylene adipate)) that grafted with polymer brushes (poly(oligoethylene glycol) methacrylate).[137]

Dynamic surfaces can also reversibly control surface properties with shape changing or two-way RSM polymers.[50,138–141] Figure 15(c–i) shows an example of dynamic surface using semicrystalline two-way RSM materials.[50] Complicated micropatterns as boomerangs or cubes can be embossed and then programmed into flat surface. Between cyclic partial melting and recrystallization, the micro features would rise in height upon heating and shrink lower upon cooling reversibly for multiple cycles. Contact angles can be controlled by the reversible surface pattern variation.

Switchable surface microstructures can lead to controllable optical properties and potential application in optical devices.[51,142,143] The intensity modulation of a diffraction grating utilizing two-way RSM was reported by Tippets

et al.[51] Periodic grating was programmed on semicrystalline poly(octylene adipate) films.

The reversible shifting of the grating height was accomplished through partial melting and recrystallization. Upon heating, the gratings partially recover to their original shape as the height of the gratings decreases, resulting in decrease in diffraction intensity, cooling and recrystallization lead to increase in grating height and higher diffraction intensity. The cyclic optical property change can be controlled by choice of partial melting temperature (Fig. 16).

CONCLUSION

This review presents a summary of different concepts for reversible shape-shifting in polymeric materials. Demands in potential applications from microrobotics to biomedical devices require materials that capable of reversibly actuating between sophisticated shapes, from macro- to nanoscales and within variety of environments under different stimuli. The challenge was met with development through both chemical designs with synthetically new materials and novel mechanisms and protocols that expand the applications of existing polymers. The advances show promising future for smart materials that could change our daily life.

ACKNOWLEDGMENT

We gratefully acknowledge funding from the National Science Foundation (DMR 1122483, DMR 1407645, and DMR 1436201).

REFERENCES AND NOTES

1 K. Otsuka, X. B. Ren, *Intermetallics* **1999**, *7*, 511–528.

2 L. G. Machado, M. A. Savi, *Braz. J. Med. Biol. Res.* **2003**, *36*, 683–691.

3 S. Miyazaki, K. Otsuka, *ISIJ Int.* **1989**, *29*, 353–377.

4 N. B. Morgan, *Mater. Sci. Eng. A: Struct. Mater. Prop. Microstruct. Process.* **2004**, *378*, 16–23.

5 D. J. Hartl, D. C. Lagoudas, *Proc. Inst. Mechanical Eng. Part G-J: Aerospace Eng.* **2007**, *221*, 535–552.

6 M. Behl, A. Lendlein, *Mater. Today.* **2007**, *10*, 20–28.

7 C. Liu, H. Qin, P. T. Mather, *J. Mater. Chem.* **2007**, *17*, 1543–1558.

8 P. T. Mather, X. F. Luo, I. A. Rousseau, *Annu. Rev. Mater. Res.* **2009**, *39*, 445–471.

9 M. Behl, M. Y. Razzaq, A. Lendlein, *Adv. Mater.* **2010**, *22*, 3388–3410.

10 J. L. Hu, S. J. Chen, *J. Mater. Chem.* **2010**, *20*, 3346–3355.

11 A. Lendlein, T. Sauter, *Macromol. Chem. Phys.* **2013**, *214*, 1175–1177.

12 H. Meng, G. Q. Li, *Polymer* **2013**, *54*, 2199–2221.

13 L. Sun, W. M. Huang, C. C. Wang, Z. Ding, Y. Zhao, C. Tang, and X. Y. Gao, *Liq. Cryst.* **2014**, *41*, 277–289.

14 L. Ionov, *Langmuir* **2015**, *31*, 5015–5024.

15 G. J. Berg, M. K. McBride, C. Wang, C. N. Bowman, *Polymer* **2014**, *55*, 5849–5872.

16 A. Lendlein, H. Y. Jiang, O. Junger, R. Langer, *Nature* **2005**, *434*, 879–882.

17 H. B. Lu, W. M. Huang, Y. T. Yao, *Pigm. Resin Technol.* **2013**, *42*, 237–246.

18 J. Thevenot, H. Oliveira, O. Sandre, S. Lecommandoux, *Chem. Soc. Rev.* **2013**, *42*, 7099–7116.

19 D. Habault, H. J. Zhang, Y. Zhao, *Chem. Soc. Rev.* **2013**, *42*, 7244–7256.

20 Y. Yang, W. Zhan, R. Peng, C. He, X. Pang, D. Shi, T. Jiang, and Z. Lin, *Adv. Mater.* **2015**, *27*, 6376.

21 R. R. Kohlmeyer, J. Chen, *Angew. Chem. Int. Ed.* **2013**, *52*, 9234–9237.

22 H. Wang, Y. Wang, B. C-K. Tee, Kim, Kwanpyo, J. Lopez, W. Cai, and Z. Bao, *Adv. Sci.* electronic source: DOI: 10.1002/advs.201500103, **2015**, *2*.

23 K. Gall, M. L. Dunn, Y. P. Liu, D. Finch, M. Lake, and N. A. Munshi, *Acta Mater.* **2002**, *50*, 5115–5126.

24 Z. Q. Yang, W. T. S. Huck, S. M. Clarke, A. R. Tajbakhsh, E. M. Terentjev, *Nat. Mater.* **2005**, *4*, 486–490.

25 J. M. G. Swann, P. D. Topham, *Polymers* **2010**, *2*, 454–469.

26 V. Kozlovskaya, W. Higgins, J. Chen, E. Kharlampieva, *Chem. Commun.* **2011**, *47*, 8352–8354.

27 V. Kozlovskaya, Y. Wang, W. Higgins, J. Chen, Y. Chen, and E. Kharlampieva, *Soft Matter* **2012**, *8*, 9828–9839.

28 V. Kozlovskaya, J. F. Alexander, Y. Wang, T. Kuncewicz, X. W. Liu, B. Godin, and E. Khariampieva, *ACS Nano* **2014**, *8*, 5725–5737.

29 A. Buguin, M. H. Li, P. Silberzan, B. Ladoux, P. Keller, *J. Am. Chem. Soc.* **2006**, *128*, 1088–1089.

30 H. Yang, G. Ye, X. G. Wang, P. Keller, *Soft Matter* **2011**, *7*, 815–823.

31 Y. Osada, A. Matsuda, *Nature* **1995**, *376*, 219-219

32 T. Mitsumata, J. P. Gong, Y. Osada, *Polym. Adv. Technol.* **2001**, *12*, 136–150.

33 J. K. Hao, R. A. Weiss, *ACS Macro Lett.* **2013**, *2*, 86–89.

34 Y. Y. Huang, J. Biggins, Y. Ji, E. M. Terentjev, *J. Appl. Phys.* **2010**, *107*, electronic source: DOI: 10.1063/1.3374474.

35 M. M. Ma, L. Guo, D. G. Anderson, R. Langer, *Science* **2013**, *339*, 186–189.

36 Y. J. Liu, H. Y. Du, L. W. Liu, J. S. Leng, *Smart Mater. Struct.* **2014**, *23*,

37 P. J. Skrzeszewska, L. N. Jong, F. A. de Wolf, M. A. C. Stuart, J. van der Gucht, *Biomacromolecules* **2011**, *12*, 2285–2292.

38 A. Lendlein, M. Behl, *Smart Mater. Micro/Nanosyst.* **2009**, *54*, 96–102.

39 A. Sharma, A. Neshat, C. J. Mahnen, A. D. Nielsen, J. Snyder, T. L. Stankovich, B. G. Daum, E. M. LaSpina, G. Beltrano, Y. Gao, S. Li, B?W. Park, R. J. Clements, E. J. Freeman, C. Malcuit, J. A. McDonough, L. T. J. Korley, T. Hegmann, and E. Hegmann, *Macromol. Biosci.* **2015**, *15*, 200–214.

40 A. Agrawal, O. Adetiba, H. Kim, H. Chen, J. G. Jacot, and R. Verduzco, *J. Mater. Res.* **2015**, *30*, 453–462.

41 M. Behl, J. Zotzmann, A. Lendlein, In Advances in Polymer Science, 2010; Vol. 226, A. Lendlein, Springer Berlin Heidelberg, pp *1-40*.

42 T. Chung, A. Rorno-Uribe, P. T. Mather, *Macromolecules* **2008**, *41*, 184–192.

43 J. J. Li, W. R. Rodgers, T. Xie, *Polymer* **2011**, *52*, 5320–5325.

44 K. K. Westbrook, P. T. Mather, V. Parakh, M. L. Dunn, Q. Ge, B. M. Lee, and H. J. Qi, *Smart Mater. Struct.* **2011**, *20*. electronic source: DOI: 10.1088/0964-1726/20/6/065010.

45 S. Pandini, S. Passera, M. Messori, K. Paderni, M. Toselli, A. Gianoncelli, E. Bontempi, and T. Ricco, *Polymer* **2012**, *53*, 1915–1924.

46 M. Behl, K. Kratz, U. Noechel, T. Sauter, A. Lendlein, *Proc. Natl. Acad. Sci. USA* **2013**, *110*, 12555–12559.

47 M. Behl, K. Kratz, J. Zotzmann, U. Nochel, A. Lendlein, *Adv. Mater.* **2013**, *25*, 4466–4469.

48 J. Zhou, S. A. Turner, S. M. Brosnan, Q. X. Li, J. M. Y. Carrillo, D. Nykypanchuk, O. Gang, V. S. Ashby, A. V. Dobrynin, and S. S. Sheiko, *Macromolecules* **2014**, *47*, 1768–1776.

49 Y. Meng, J. S. Jiang, M. Anthamatten, *ACS Macro Lett.* **2015**, *4*, 115–118.

50 S. A. Turner, J. Zhou, S. S. Sheiko, V. S. Ashby, *ACS Appl. Mater. Interfaces* **2014**, *6*, 8017–8021.

51 C. A. Tippets, Q. X. Li, Y. L. Fu, E. U. Donev, J. Zhou, S. A. Turner, A. M. S. Jackson, V. S. Ashby, S. S. Sheiko, and R. Lopez, *ACS Appl. Mater. Interfaces* **2015**, *7*, 14288–14293.

52 T. Gong, K. Zhao, W. X. Wang, H. M. Chen, L. Wang, and S. B. Zhou, *J. Mater. Chem. B* **2014**, *2*, 6855–6866.

53 A. R. Tajbakhsh, E. M. Terentjev, *Eur. Phys. J. E* **2001**, *6*, 181–188.

54 R. Ishige, K. Osada, H. Tagawa, H. Niwano, M. Tokita, and J. Watanabe, *Macromolecules* **2008**, *41*, 7566–7570.

55 K. D. Harris, R. Cuypers, P. Scheibe, van C. L. Oosten, C. W. M. Bastiaansen, J. Lub, and D. J. Broer, *J. Mater. Chem.* **2005**, *15*, 5043–5048.

56 W. Deng, M. H. Li, X. G. Wang, P. Keller, *Liq. Cryst.* **2009**, *36*, 1023–1029.

57 Z. Yan, X. M. Ji, W. Wu, J. Wei, Y. L. Yu, *Macromol. Rapid Commun.* **2012**, *33*, 1362–1367.

58 H. F. Yu, Q. Li, In Intelligent Stimuli-Responsive Materials: from Well-Defined Nanostructures to Applications, Q. Li, Ed.; Blackwell Science Publ, John Wiley & Sons, **2013**; pp 233–264.

59 R. B. Wei, H. X. Zhang, Y. N. He, X. G. Wang, P. Keller, *Liq. Cryst.* **2014**, *41*, 1821–1830.

60 J. A. Lv, W. Wang, W. Wu, Y. L. Yu, *J. Mater. Chem. C* **2015**, *3*, 6621–6626.

61 K. Urayama, H. Kondo, Y. O. Arai, T. Takigawa, *Phys. Rev. E* **2005**, *71*, electronic source: DOI: 10.1103/PhysRevE.71.051713.

62 S. Maeda, Y. Hara, T. Sakai, R. Yoshida, S. Hashimoto, *Adv. Mater.* **2007**, *19*, 3480 +,

63 C. Yang, W. Wang, C. Yao, R. Xie, X. J. Ju, Z. Liu, and L. Y. Chu, *Sci. Rep.* **2015**, *5*, electronic source: DOI: 10.1038/srep13622.

64 D. Szabo, G. Szeghy, M. Zrinyi, *Macromolecules* **1998**, *31*, 6541–6548.

65 J. Lu, S. G. Kim, S. Lee, I. K. Oh, *Adv. Funct. Mater.* **2008**, *18*, 1290–1298.

66 J. Lu, S. G. Kim, S. Lee, I. K. Oh, In Conference on Electroactive Polymer Actuators and Devices (EAPAD 2008). Spie-Int Soc Optical Engineering, EAPAD 2008, San Diego, California, USA, **2008**.

67 Q. Yu, J. M. Bauer, J. S. Moore, D. J. Beebe, *Appl. Phys. Lett.* **2001**, *78*, 2589–2591.

68 H. Meng, G. Q. Li, *J. Mater. Chem. A* **2013**, *1*, 7838–7865.

69 S. Varghese, A. K. Lele, D. Srinivas, M. Sastry, R. A. Mashelkar, *Adv. Mater.* **2001**, *13*, 1544 +,

70 W. Guo, C-H. Lu, R. Orbach, F. Wang, X-J. Qi, A. Cecconello, D. Seliktar, and I. Willner, *Adv. Mater.* **2015**, *27*, 73–78.

71 Y. L. Yu, M. Nakano, T. Ikeda, *Nature* **2003**, *425*, 145–145.

72 H. F. Yu, T. Ikeda, *Adv. Mater.* **2011**, *23*, 2149–2180.

73 M. H. Li, A. Brulet, J. P. Cotton, P. Davidson, C. Strazielle, and P. Keller, *J. De Phys. Ii.* **1994**, *4*, 1843–1863.

74 F. Hardouin, G. Sigaud, M. F. Achard, A. Brulet, J. P. Cotton, D. Y. Yoon, V. Percec, and M. Kawasumi, *Macromolecules* **1995**, *28*, 5427–5433.

75 T. J. White, D. J. Broer, *Nat. Mater.* **2015**, *14*, 1087–1098.

76 H. R. Jiang, C. S. Li, X. Z. Huang, *Nanoscale* **2013**, *5*, 5225–5240.

77 E. K. Fleischmann, R. Zentel, *Angew. Chem. Int. Ed.* **2013**, *52*, 8810–8827.

78 W. Wu, J. Shen, P. Banerjee, S. Q. Zhou, *Biomaterials* **2010**, *31*, 8371–8381.

79 Y. L. Yu, T. Ikeda, *Angew. Chem. Int. Ed.* **2006**, *45*, 5416–5418.

80 W. X. Xu, R. Y. Yin, L. Lin, Y. Yu, *Prog. Chem.* **2008**, *20*, 140–147.

81 C. Ohm, M. Brehmer, R. Zentel, *Adv. Mater.* **2010**, *22*, 3366–3387.

82 C. Ohm, C. Serra, R. Zentel, *Adv. Mater.* **2009**, *21*, 4859 +.

83 Z. Q. Pei, Y. Yang, Q. M. Chen, E. M. Terentjev, Y. Wei, and Y. Ji, *Nat. Mater.* **2014**, *13*, 36–41.

84 E. K. Fleischmann, F. R. Forst, K. Koder, N. Kapernaum, R. Zentel, *J. Mater. Chem. C* **2013**, *1*, 5885–5891.

85 M. H. Li, P. Keller, *Philos. Trans. R. Soc. A: Math. Phys. Eng. Sci.* **2006**, *364*, 2763–2777.

86 T. Mirfakhrai, J. D. W. Madden, R. H. Baughman, *Mater. Today* **2007**, *10*, 30–38.

87 M. R. Islam, X. Li, K. Smyth, M. J. Serpe, *Angew. Chem. Int. Ed.* **2013**, *52*, 10330–10333.

88 P. Ariano, D. Accardo, M. Lombardi, S. Bocchini, L. Draghi, D. e. L. Nardo, and P. Fino, *J. Appl. Biomater. Funct. Mater.* **2015**, *13*, 1–9.

89 X. Li, M. J. Serpe, *Adv. Funct. Mater.* **2014**, *24*, 4119–4126.

90 M. H. Li, P. Keller, J. Y. Yang, P. A. Albouy, *Adv. Mater.* **2004**, *16*, 1922 +.

91 M. H. Li, A. Brulet, P. Davidson, P. Keller, J. P. Cotton, *Phys. Rev. Lett.* **1993**, *70*, 2297–2300.

92 M. Dai, O. T. Picot, J. M. N. Verjans, de L. T. Haan, A. Schenning, T. Peijs, and C. W. M. Bastiaansen, *ACS Appl. Mater. Interfaces* **2013**, *5*, 4945–4950.

93 Z. L. Wu, M. Moshe, J. Greener, Therien-Aubin H., Z. H. Nie, E. Sharon, and E. Kumacheva, *Nat. Commun.* **2013**, *4*. electronic source: DOI: 10.1038/ncomms2549.

94 H. Therien-Aubin, M. Moshe, E. Sharon, E. Kumacheva, *Soft Matter* **2015**, *11*, 4600–4605.

95 de L. T. Haan, Gimenez-Pinto V., A. Konya, T. S. Nguyen, J. M. N. Verjans, Sanchez-Somolinos C., J. V. Selinger, R. L. B. Selinger, D. J. Broer, and A. Schenning, *Adv. Funct. Mater.* **2014**, *24*, 1251–1258.

96 C. X. Ma, T. F. Li, Q. Zhao, X. X. Yang, J. J. Wu, Y. W. Luo, and T. Xie, *Adv. Mater.* **2014**, *26*, 5665.

97 R. Verduzco, *Science* **2015**, *347*, 949–950.

98 T. H. Ware, M. E. McConney, J. J. Wie, V. P. Tondiglia, T. J. White, *Science* **2015**, *347*, 982–984.

99 J. R. Kumpfer, S. J. Rowan, *J. Am. Chem. Soc.* **2011**, *133*, 12866–12874.

100 J. Mendez, P. K. Annamalai, S. J. Eichhorn, R. Rusli, S. J. Rowan, E. J. Foster, and C. Weder, *Macromolecules* **2011**, *44*, 6827–6835.

101 B. T. Michal, B. M. McKenzie, S. E. Felder, S. J. Rowan, *Macromolecules* **2015**, *48*, 3239–3246.

102 W. J. Nan, W. Wang, H. Gao, W. G. Liu, *Soft Matter* **2013**, *9*, 132–137.

103 B. Xu, Y. Y. Zhang, W. G. Liu, *Macromol. Rapid Commun.* **2015**, *36*, 1585–1591.

104 Q. Ge, C. K. Dunn, H. J. Qi, M. L. Dunn, *Smart Mater. Struct.* **2014**, *23*, 15, electronic source: DOI: 10.1088/0964-1726/23/9/094007

105 Q. Ge, H. J. Qi, M. L. Dunn, *Appl. Phys. Lett.* **2013**, *103*, electronic source: DOI: 10.1063/1.4819837.

106 Y. Q. Mao, K. Yu, M. S. Isakov, J. T. Wu, M. L. Dunn, and H. J. Qi, *Sci. Rep.* **2015**, *5*, electronic source: DOI: 10.1038/srep13616.

107 S. Tibbits, C. McKnelly, C. Olguin, D. Dikovsky, S. Hirsch, *Acadia 2014: Des. Agency* **2014**, 539–548.

108 E. J. Pei, *Assembly Autom.* **2014**, *34*, 310–314.

109 J. Zhou, Q. X. Li, S. A. Turner, V. S. Ashby, S. S. Sheiko, *Polymer* **2015**, *72*, 464–470.

110 I. Bellin, S. Kelch, R. Langer, A. Lendlein, *Proc. Natl. Acad. Sci. USA* **2006**, *103*, 18043–18047.

111 T. Xie, X. C. Xiao, Y. T. Cheng, *Macromol. Rapid Commun.* **2009**, *30*, 1823–1827.

112 M. Behl, A. Lendlein, *J. Mater. Chem.* **2010**, *20*, 3335–3345.

113 Y. W. Luo, Y. L. Guo, X. Gao, B. G. Li, T. Xie, *Adv. Mater.* **2013**, *25*, 743–748.

114 T. Xie, *Nature* **2010**, *464*, 267–270.

115 K. Kratz, S. A. Madbouly, W. Wagermaier, A. Lendlein, *Adv. Mater.* **2011**, *23*, 4058 +.

116 K. Kratz, U. Voigt, A. Lendlein, *Adv. Funct. Mater.* **2012**, *22*, 3057–3065.

117 K. Yu, T. Xie, J. S. Leng, Y. F. Ding, H. J. Qi, *Soft Matter* **2012**, *8*, 5687–5695.

118 R. D. Andrews, A. V. Tobolsky, E. E. Hanson, *J. Appl. Phys.* **1946**, *17*, 352–361.

119 M. Behl, J. Zotzmann, A. Lendlein, *Int. J. Artif. Organs* **2011**, *34*, 231–237.

120 S. J. Chen, J. L. Hu, H. T. Zhuo, *Compos. Sci. Technol.* **2010**, *70*, 1437–1443.

121 S. J. Chen, J. L. Hu, H. T. Zhuo, Y. Zhu, *Mater. Lett.* **2008**, *62*, 4088–4090.

122 A. Basit, G. L'Hostis, M. J. Pac, B. Durand, *Materials* **2013**, *6*, 4031–4045.

123 Q. Ge, K. K. Westbrook, P. T. Mather, M. L. Dunn, H. J. Qi, *Smart Mater. Struct.* **2013**, *22*, electronic source: DOI: 10.1088/0964-1726/22/5/055009.

124 M. Saatchi, M. Behl, U. Nochel, A. Lendlein, *Macromol. Rapid Commun.* **2015**, *36*, 880–884.

125 V. Stroganov, Al-Hussein M., J. U. Sommer, A. Janke, S. Zakharchenko, and L. Ionov, *Nano Lett.* **2015**, *15*, 1786–1790.

126 S. Kim, C. Laschi, B. Trimmer, *Trends Biotechnol.* **2013**, *31*, 23–30.

127 M. Camacho-Lopez, H. Finkelmann, P. Palffy-Muhoray, M. Shelley, *Nat. Mater.* **2004**, *3*, 307–310.

128 Y. Ueoka, J. Gong, Y. Osada, *J. Intell. Mater. Syst. Struct.* **1997**, *8*, 465–471.

129 D. Morales, E. Palleau, M. D. Dickey, O. D. Velev, *Soft Matter* **2014**, *10*, 1337–1348.

130 K. A. Davis, K. A. Burke, P. T. Mather, J. H. Henderson, *Biomaterials* **2011**, *32*, 2285–2293.

131 D. M. Le, K. Kulangara, A. F. Adler, K. W. Leong, V. S. Ashby, *Adv. Mater.* **2011**, *23*, 3278.

132 J. Li, J. M. Shim, J. Deng, J. T. B. Overvelde, X. L. Zhu, K. Bertoldi, and S. Yang, *Soft Matter* **2012**, *8*, 10322–10328.

133 S. M. Brosnan, A. H. Brown, V. S. Ashby, *J. Am. Chem. Soc.* **2013**, *135*, 3067–3072.

134 M. Ebara, K. Uto, N. Idota, J. M. Hoffman, T. Aoyagi, *Adv. Mater.* **2012**, *24*, 273–278.

135 N. Bowden, S. Brittain, A. G. Evans, J. W. Hutchinson, G. M. Whitesides, *Nature* **1998**, *393*, 146–149.

136 S. Yang, K. Khare, P. C. Lin, *Adv. Funct. Mater.* **2010**, *20*, 2550–2564.

137 A. M. S. Jackson, S. S. Sheiko, V. S. Ashby, *Langmuir* **2015**, *31*, 5489–5494.

138 C. L. Feng, Y. J. Zhang, J. Jin, Y. L. Song, L. Y. Xie, G. R. Qu, L. Jiang, and D. B. Zhu, *Langmuir* **2001**, *17*, 4593–4597.

139 T. L. Sun, G. J. Wang, L. Feng, B. Q. Liu, Y. M. Ma, L. Jiang, and D. B. Zhu, *Angew. Chem. Int. Ed.* **2004**, *43*, 357–360.

140 Z. L. Wu, R. B. Wei, A. Buguin, J. M. Taulemesse, N. Le Moigne, T. A. Bergere, X. G. Wang, and P. Keller, *ACS Appl. Mater. Interfaces* **2013**, *5*, 7485–7491.

141 J. D. Eisenhaure, T. Xie, S. Varghese, S. Kim, *ACS Appl. Mater. Interfaces* **2013**, *5*, 7714–7717.

142 H. X. Xu, C. J. Yu, S. D. Wang, V. Malyarchuk, T. Xie, and J. A. Rogers, *Adv. Funct. Mater.* **2013**, *23*, 3299–3306.

143 R. B. Wei, Y. N. He, X. G. Wang, P. Keller, *Macromol. Rapid Commun.* **2013**, *34*, 330–334.